Research Article

Pedestrian Walking Behavior Revealed through a Random Walk Model

Hui Xiong, Liya Yao, Huachun Tan, and Wuhong Wang

Department of Transportation Engineering, Beijing Institute of Technology, Beijing 100084, China

Correspondence should be addressed to Hui Xiong, xionghui@bit.edu.cn

This paper applies method of continuous-time random walks for pedestrian flow simulation. In the model, pedestrians can walk forward or backward and turn left or right if there is no block. Velocities of pedestrian flow moving forward or diffusing are dominated by coefficients. The waiting time preceding each jump is assumed to follow an exponential distribution. To solve the model, a second-order two-dimensional partial differential equation, a high-order compact scheme with the alternating direction implicit method, is employed. In the numerical experiments, the walking domain of the first one is two-dimensional with two entrances and one exit, and that of the second one is two-dimensional with one entrance and one exit. The flows in both scenarios are one way. Numerical results show that the model can be used for pedestrian flow simulation.

1. Introduction

In recent years, modeling pedestrian flow has attracted considerable attention, partly because the model serves as basis for efficient crowd evacuation management and pedestrian facility operations. However, the research is still in its infancy owing to the complexity of human being's behaviors.

Most of the existing models for pedestrian flow are of microscopic nature, describing in detail the interactions among pedestrians, and between pedestrians and obstacles. Those models include, among others, cellular automata models [1–7], lattice gas models [8–12], the social force models [13], the centrifugal force models [14], and the floor field models [15, 16]. In cellular automata models, the walking space is two-dimensional and divided into cells. Each cell can either be empty, be occupied by exactly one pedestrian, or contain an obstacle. Cellular automata models are widely used for capturing pedestrian walking behaviors, such as bi-direction movement [1, 3, 4], pedestrian counter flow with different walk velocities

[2] or with right-moving preference [5], freezing transition phenomenon [6], and moving pedestrians' reaction to an obstacle [7]. Like cellular automata models, the lattice gas model consists of a set of stochastic rules on the square lattice. Applying the lattice gas model, previous studies have systematically investigated the phenomenon of jamming transition from the moving state at a low density to the stopping state at a higher density [8–11]. Jiang and Wu employed the lattice gas model to examine the interaction between a large object and pedestrians in the narrow channel [12]. The social force model, proposed by Helbing and Molnár [13], consists of three force terms that are measures for the moving motivations of a pedestrian. The model is able to reproduce the self-organization of collective phenomena of walking behaviors. By considering the headway and relative velocity among pedestrians, the centrifugal force model is capable of describing the behavior of lane formation [14]. The floor field model is yet another type of cellular automata models extended by realistically taking into account pedestrians' behaviors around the exit [15, 16].

Macroscopic models are often in the form of partial differential equations. Instead of describing individual pedestrian's behavior, this type of models treats the crowd as a whole and applies the conservation laws to capture the relationship among speed, flow, and density of pedestrian flow [17–21]. Directly starting from the flow conservation, Hughes [17] derived partial differential equations for flows with single or multiple pedestrian types. Likewise, Colombo and Rosini [18] introduced another partial differential equation model for pedestrian flows with a new parameter called characteristic density, which is used to reveal the maximal density in panic. Henderson [19] considered the movement of a crowd as an analogous system of gas molecules and applied the Maxwell-Boltzmann theory to describe the velocity distribution of people movements. Without making use of the conservation assumptions in Henderson's study, Helbing [20] developed a fluid dynamic model for the collective movement of pedestrians based on the Boltzmann-like approach.

Motivated by the work by Barkai et al. [22], this paper attempts to apply the approach of continuous-time random walks (CTRW) to derive a partial differential equation model to describe the motion of pedestrians. The CTRW is a useful model from statistical physics, in which each random particle jump is preceded by a random waiting time. Mathematically, the CTRW is a random walk subordinated to a renewal process. Different from the traditional macroscopic models, the proposed model is capable of not only capturing the macroscopic characteristics of pedestrian flows, but also describing the interactions among pedestrians, and between pedestrians and obstacles in terms of parameters in the model.

This paper is organized as follows. Section 2 introduces the continuous-time random walks model, formulated as a partial differential equation. Section 3 presents a high-order compact (HOC) solution scheme with the alternating direction implicit (ADI) method, followed by a numerical example in Section 4. Finally, Section 5 concludes the paper.

2. Model

Consider a random walker on a bounded two-dimensional lattice with a domain $\Omega \in R^2$. It is assumed that there is no correlation between steps. Let τ represent the time that the walker stays at a particular point before making a "jump." Hereinafter we simply call τ as waiting time at a point and assume the waiting time at all points are independent random variables with an identical probability density function $\psi(\tau)$. We further define $\Psi(N, t)$

as the probability of N jumps occurring during the time interval $(0, t)$. Consequently, the probability that there is no jump occurring during the time interval $(0, t)$ is

$$\Psi(0, t) = P(\tau > t) = 1 - P(\tau \leq t) = 1 - \int_0^t \psi(\tau) d\tau. \tag{2.1}$$

Applying the Laplace transform to both sides of (2.1) leads to

$$\widetilde{\Psi}(0, s) = \frac{1 - \widetilde{\psi}(s)}{s}. \tag{2.2}$$

Note that $\Psi(1, t)$ represents the probability that the first jump occurs at time t' and there are no further jumps after it until t. We thus have

$$\Psi(1, t) = \int_0^t \psi(t') \Psi(0, t - t') dt' \overset{\text{def}}{=} \psi * \Psi, \tag{2.3}$$

where $\Psi(0, t)$ and $\psi(t)$ are simplified as Ψ and ψ. Similarly, we obtain

$$\Psi(N, t) = \psi * \psi * \psi * \cdots * \Psi = \psi^{*N} * \Psi. \tag{2.4}$$

The Laplace form of (2.4) is given by

$$\widetilde{\Psi}(N, s) = \widetilde{\psi}^N(s) \frac{1 - \widetilde{\psi}(s)}{s}. \tag{2.5}$$

Let $P(x, y, t)$ be the probability of observing the walker at site (x, y) at time t, and let $p_N(x, y)$ denote the probability that the walker is at the position (x, y) after N jumps. We then have

$$P(x, y, t) = \sum_{N=0}^{\infty} p_N(x, y) \Psi(N, t). \tag{2.6}$$

The Laplace transformation of (2.6) yields

$$\widetilde{P}(x, y, s) = \frac{1 - \widetilde{\psi}(s)}{s} \sum_{N=0}^{\infty} p_N(x, y) \widetilde{\psi}^N(s) = \frac{1 - \widetilde{\psi}(s)}{s} p_0(x, y) + \frac{1 - \widetilde{\psi}(s)}{s} \sum_{N=1}^{\infty} p_N(x, y) \widetilde{\psi}^N(s). \tag{2.7}$$

In the domain of Ω with the length of the lattice edge being h (as shown in Figure 1), the law of total probability implies that

$$p_N(x, y) = r_1 p_{N-1}(x - h, y) + r_2 p_{N-1}(x, y - h) + r_3 p_{N-1}(x + h, y) + r_4 p_{N-1}(x, y + h), \tag{2.8}$$
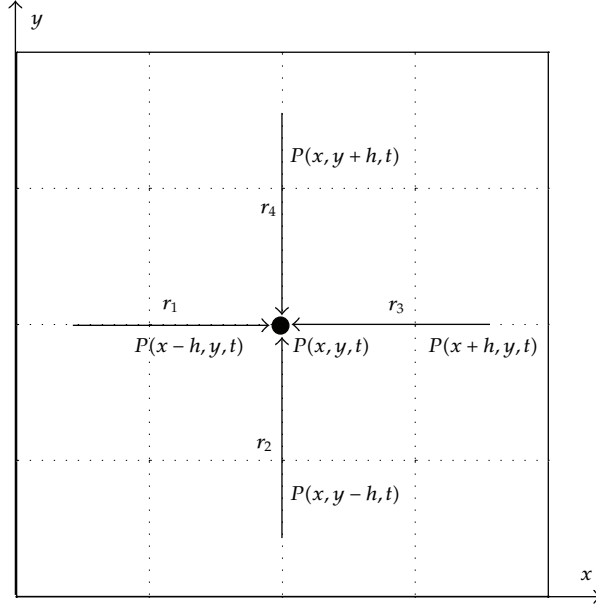
Figure 1: Probabilities of walking directions.

where r_1 to r_4 represents the probability for the walker to proceed forward, turn left, walk back, and turn right, respectively. The probabilities are assumed to be known and $\sum_{i=1}^{4} r_i = 1$.

Applying Taylor's expansion to RHS of (2.8) at the point (x, y) leads to

$$
\begin{aligned}
p_N(x, y) = r_1 & \left[p_{N-1}(x, y) - h \frac{\partial}{\partial x_1} p_{N-1}(x, y) + \frac{1}{2} h^2 \frac{\partial^2}{\partial x_1^2} p_{N-1}(x, y) \right] \\
+ r_2 & \left[p_{N-1}(x, y) - h \frac{\partial}{\partial x_2} p_{N-1}(x, y) + \frac{1}{2} h^2 \frac{\partial^2}{\partial x_2^2} p_{N-1}(x, y) \right] \\
+ r_3 & \left[p_{N-1}(x, y) + h \frac{\partial}{\partial x_1} p_{N-1}(x, y) + \frac{1}{2} h^2 \frac{\partial^2}{\partial x_1^2} p_{N-1}(x, y) \right] \\
+ r_4 & \left[p_{N-1}(x, y) + h \frac{\partial}{\partial x_2} p_{N-1}(x, y) + \frac{1}{2} h^2 \frac{\partial^2}{\partial x_2^2} p_{N-1}(x, y) \right] + O\left(h^2\right),
\end{aligned}
\tag{2.9}
$$

where $O(h^2)$ denotes higher-order terms that are omitted hereinafter. We thus obtain the following:

$$
\begin{aligned}
p_N(x, y) = p_{N-1}(x, y) & - (r_1 - r_3) h \frac{\partial}{\partial x} p_{N-1}(x, y) - (r_2 - r_4) h \frac{\partial}{\partial y} p_{N-1}(x, y) \\
& + (r_1 + r_3) \frac{h^2}{2} \frac{\partial^2}{\partial x^2} p_{N-1}(x, y) + (r_2 + r_4) \frac{h^2}{2} \frac{\partial^2}{\partial y^2} p_{N-1}(x, y).
\end{aligned}
\tag{2.10}
$$

Define $f(x) = (r_1 - r_3)/h$, $f(y) = (r_2 - r_4)/h$, where $f(x)$ is the direction force along the x-axis and $f(y)$ is the force along the y-axis. Consequently, (2.10) can be recast as

$$p_N(x,y) = p_{N-1}(x,y) - V_1 \frac{\partial}{\partial x} p_{N-1}(x,y) - V_2 \frac{\partial}{\partial y} p_{N-1}(x,y)$$

$$+ W_1 \frac{\partial^2}{\partial x^2} p_{N-1}(x,y) + W_2 \frac{\partial^2}{\partial y^2} p_{N-1}(x,y), \tag{2.11}$$

where $V_1 = h^2 f(x)$, $V_2 = h^2 f(y)$, $W_1 = (r_1 + r_3)h^2/2$, and $W_2 = (r_2 + r_4)h^2/2$. Applying the Laplace transformation to (2.11), we have

$$\tilde{p}_N(x,y) = \tilde{p}_{N-1}(x,y) + h^2 L_{FP} \tilde{p}_{N-1}(x,y), \tag{2.12}$$

where $L_{FP} = -f(x)\partial/\partial x - f(y)\partial/\partial y + (W_1/h^2)\partial^2/\partial x^2 + (W_2/h^2)\partial^2/\partial y^2$.

Substituting (2.12) into (2.7) yields

$$\tilde{P}(x,y,s) = \frac{1 - \tilde{\psi}(s)}{s} p_0(x,y) + \frac{1 - \tilde{\psi}(s)}{s} \tilde{\psi}(s) \sum_{N=0}^{\infty} \left[\tilde{p}_N(x,y) + h^2 L_{FP} \tilde{p}_N(x,y) \right] \tilde{\psi}^N(s)$$

$$= \frac{1 - \tilde{\psi}(s)}{s} p_0(x,y) + \tilde{\psi}(s) \tilde{P}(x,y,s) + \tilde{\psi}(s) h^2 L_{FP} \tilde{P}(x,y,s). \tag{2.13}$$

The specific form of (2.13) depends on the choice of the waiting time distribution $\psi(\tau)$. Several distributions are plausible based on the nature of pedestrian walking behaviors. Here we assume that $\psi(\tau)$ follows the exponential distribution, that is,

$$\psi(\tau) \sim \frac{1}{\lambda} e^{-\tau/\lambda}, \tag{2.14}$$

where λ is the mean of waiting time. The probability density function of waiting time in the Laplace space can be written as

$$\tilde{\psi}(s) = \frac{1}{1 + \lambda s} = 1 - \lambda s + \cdots. \tag{2.15}$$

Substituting (2.15) into (2.13) yields

$$\tilde{P}(x,y,s) = \lambda p_0(x,y) + (1 - \lambda s)\tilde{P}(x,y,s) + (1 - \lambda s)h^2 L_{FP} \tilde{P}(x,y,s). \tag{2.16}$$

Rearranging the above and dividing both sides by λs leads to

$$\tilde{P}(x,y,s) - \frac{1}{s} p_0(x,y) = \frac{k}{s} L_{FP} \tilde{P}(x,y,s), \tag{2.17}$$

where $k = \lim h^2/\lambda$ as $h^2 \to 0, \lambda \to 0$. Then the inverse Laplace transform of (2.17) becomes the following:

$$P(x, y, t) = kL_{FP} \int_0^t P(x, y, t)dt. \tag{2.18}$$

We thus obtain the continuous-time random walks model for pedestrian traffic as

$$\frac{\partial P(x, y, t)}{\partial t} = kL_{FP}P(x, y, t). \tag{2.19}$$

3. Numerical Algorithm

Equation (2.19) is recognized as the Fokker-Planck equation. If none of the coefficients is function of x or y, then it is a linear second-order partial differential equation. Here we employ a high-order compact scheme with the alternating direction implicit method to numerically solve this equation [23, 24]. Further denoting $(r_1 - r_3)k/h$ as β_x, $(r_2 - r_4)k/h$ as β_y, $(r_1 + r_3)k/2$ as α_x, and $(r_2 + r_4)k/2$ as α_y, we rewrite the model as follows:

$$\beta_x \frac{\partial P}{\partial x} + \beta_y \frac{\partial P}{\partial y} - \alpha_x \frac{\partial^2 P}{\partial x^2} - \alpha_y \frac{\partial^2 P}{\partial y^2} = -\frac{\partial P}{\partial t}. \tag{3.1}$$

Assume the domain Ω is divided evenly into spaced cells of length Δx along x-axis and length Δy along y-axis, and $\delta_x P_{ij}$, $\delta_y P_{ij}$, $\delta_x^2 P_{ij}$, and $\delta_y^2 P_{ij}$ represent the approximations to the first and second derivatives of P with respect to x or y at node (x_i, y_j). Based on the standard central finite difference method, (3.1) can be discretized as follows:

$$\beta_x \delta_x P_{ij} + \beta_y \delta_y P_{ij} - \alpha_x \delta_x^2 P_{ij} - \alpha_y \delta_y^2 P_{ij} - \tau_{ij} = -\frac{\partial P}{\partial t}\bigg|_{ij}. \tag{3.2}$$

In the above, the truncation error, that is, τ_{ij}, is

$$\tau_{ij} = \left[\beta_x \frac{\Delta x^2}{6} \delta_x^3 + \beta_y \frac{\Delta y^2}{6} \delta_y^3 - \alpha_x \frac{\Delta x^2}{12} \delta_x^4 - \alpha_y \frac{\Delta y^2}{12} \delta_y^4\right] P_{ij} + O\left(\Delta x^4 + \Delta y^4\right), \tag{3.3}$$

where δ_x, δ_y, δ_x^2, and δ_y^2 are the first- and second-order central difference operators.

Differentiating (3.1) with respect to x or y once and twice, respectively yields, approximations of higher-order derivatives as follows:

$$\delta_x^3 P_{ij} = \left[\left(\frac{\beta_y}{\alpha_x} \delta_y - \frac{\alpha_y}{\alpha_x} \delta_y^2 \right) \delta_x + \frac{\beta_x}{\alpha_x} \delta_x^2 + \frac{1}{\alpha_x} \delta_x \delta_t \right] P_{ij} + O\left(\Delta x^4 + \Delta y^4 \right),$$

$$\delta_y^3 P_{ij} = \left[\left(\frac{\beta_x}{\alpha_y} \delta_x - \frac{\alpha_x}{\alpha_y} \delta_x^2 \right) \delta_y + \frac{\beta_y}{\alpha_y} \delta_y^2 + \frac{1}{\alpha_y} \delta_y \delta_t \right] P_{ij} + O\left(\Delta x^4 + \Delta y^4 \right),$$

$$\delta_x^4 P_{ij} = \left[\left(\frac{\beta_x \beta_y}{\alpha_x^2} \delta_y - \frac{\alpha_y \beta_x}{\alpha_x^2} \delta_y^2 \right) \delta_x + \left(\frac{\beta_x^2}{\alpha_x^2} + \frac{\beta_y}{\alpha_x} \delta_y - \frac{\alpha_y}{\alpha_x} \delta_y^2 \right) \delta_x^2 + \left(\frac{\beta_x}{\alpha_x^2} \delta_x + \frac{1}{\alpha_x} \delta_x^2 \right) \delta_t \right] P_{ij} \tag{3.4}$$
$$+ O\left(\Delta x^4 + \Delta y^4 \right),$$

$$\delta_y^4 P_{ij} = \left[\left(\frac{\beta_x \beta_y}{\alpha_y^2} \delta_x - \frac{\alpha_x \beta_y}{\alpha_y^2} \delta_x^2 \right) \delta_y + \left(\frac{\beta_y^2}{\alpha_y^2} + \frac{\beta_x}{\alpha_y} \delta_x - \frac{\alpha_x}{\alpha_y} \delta_x^2 \right) \delta_y^2 + \left(\frac{\beta_y}{\alpha_y^2} \delta_y + \frac{1}{\alpha_y} \delta_y^2 \right) \delta_t \right] P_{ij}$$
$$+ O\left(\Delta x^4 + \Delta y^4 \right).$$

Substituting (3.4) and (3.3) into (3.2) leads to

$$\left[\beta_x \delta_x + \beta_y \delta_y - A \delta_x^2 - B \delta_y^2 - C \delta_x \delta_y + D \delta_x \delta_y^2 + E \delta_x^2 \delta_y + F \delta_x^2 \delta_y^2 \right] P_{ij} = G \delta_t P_{ij} + O\left(\Delta x^4 + \Delta y^4 \right), \tag{3.5}$$

where $A = \alpha_x - \beta_x^2 \Delta x^2 / 12\alpha_x$, $B = \alpha_y - \beta_y^2 \Delta y^2 / 12\alpha_y$, $C = \beta_x \beta_y \Delta x^2 / 12\alpha_x + \beta_x \beta_y \Delta y^2 / 12\alpha_y$, $D = \alpha_y \beta_x \Delta x^2 / 12\alpha_x + \beta_x \Delta y^2 / 12$, $E = \alpha_x \beta_y \Delta y^2 / 12\alpha_y + \Delta x^2 \beta_y / 12$, $F = \alpha_x \Delta y^2 / 12 - \alpha_y \Delta x^2 / 12$, and $G = -1 + (\beta_x \Delta x^2 / 12\alpha_x)\delta_x + (\beta_y \Delta y^2 / 12\alpha_y)\delta_y - (\Delta x^2 / 12)\delta_x^2 - (\Delta y^2 / 12)\delta_y^2$.

Following Karaa and Zhang [24], we define four finite difference operators,

$$L_x = 1 + \frac{\Delta x^2}{12} \left(\delta_x^2 - \frac{\beta_x}{\alpha_x} \delta_x \right), \qquad L_y = 1 + \frac{\Delta y^2}{12} \left(\delta_y^2 - \frac{\beta_y}{\alpha_y} \delta_y \right),$$
$$A_x = -\left(\alpha_x + \frac{\beta_x^2 \Delta x^2}{12\alpha_x} \right) \delta_x^2 + \beta_x \delta_x, \qquad A_y = -\left(\alpha_y + \frac{\beta_y^2 \Delta y^2}{12\alpha_y} \right) \delta_y^2 + \beta_y \delta_y. \tag{3.6}$$

The difference between LHS of (3.5) and $(L_x A_y + L_y A_x) P_{ij}$ is expressed as

$$\left[\frac{\beta_x^2 \beta_y \Delta x^2 \Delta y^2}{144 \alpha_x \alpha_y} \delta_x^2 \delta_y + \frac{\beta_x \beta_y^2 \Delta x^2 \Delta y^2}{144 \alpha_x \alpha_y} \delta_x \delta_y^2 - \left(\frac{\beta_x^2 \Delta x^2 \Delta y^2}{144 \alpha_x} + \frac{\beta_y^2 \Delta x^2 \Delta y^2}{144 \alpha_y} \right) \delta_x^2 \delta_y^2 \right] P_{ij}, \tag{3.7}$$

while the difference between RHS of (3.5) and $L_x L_y \delta_t P_{ij}$ is

$$\left[\frac{\beta_x \beta_y \Delta x^2 \Delta y^2}{144 \alpha_x \alpha_y} \delta_x \delta_y - \frac{\beta_x \Delta x^2 \Delta y^2}{144 \alpha_x} \delta_x \delta_y^2 - \frac{\beta_y \Delta x^2 \Delta y^2}{144 \alpha_y} \delta_x^2 \delta_y + \frac{\Delta x^2 \Delta y^2}{144} \delta_x^2 \delta_y^2 \right] \delta_t P_{ij}. \tag{3.8}$$

Thus (3.5) can be rewritten as

$$[L_x A_y + L_y A_x] P_{ij} = L_x L_y \delta_t P_{ij} + O\left(\Delta x^4 + \Delta y^4\right), \tag{3.9}$$

since adding the above two expressions to (3.5) will not influence the accuracy. Applying the Crank-Nicolson discretization, we have

$$(L_x A_y + L_y A_x) \frac{P_{ij}^{n+1} + P_{ij}^n}{2} = -L_x L_y \frac{P_{ij}^{n+1} - P_{ij}^n}{\Delta t} + O\left(\Delta x^4 + \Delta y^4\right) + O\left(\Delta t^2\right). \tag{3.10}$$

This discretization is apparently second order in time and fourth order in space.

We move the terms with P_{ij}^{n+1} in the above equation to its LHS and add $\Delta t^2 A_x A_y P_{ij}^{n+1}/4$ to it. Similarly, we move the terms with P_{ij}^n to the RHS and add $\Delta t^2 A_x A_y P_{ij}^n/4$. Consequently, (3.10) becomes the following equation after dropping the error terms [24]:

$$\left(L_x + \frac{\Delta t}{2} A_x\right)\left(L_y + \frac{\Delta t}{2} A_y\right) u_{ij}^{n+1} = \left(L_x - \frac{\Delta t}{2} A_x\right)\left(L_y - \frac{\Delta t}{2} A_y\right) P_{ij}^n. \tag{3.11}$$

Employing the alternating direction implicit method, we have

$$\left(L_x + \frac{\Delta t}{2} A_x\right) P_{ij}^{n+1/2} = \left(L_x - \frac{\Delta t}{2} A_x\right)\left(L_y - \frac{\Delta t}{2} A_y\right) P_{ij}^n,$$

$$\left(L_y + \frac{\Delta t}{2} A_y\right) P_{ij}^{n+1} = P_{ij}^{n+1/2}, \tag{3.12}$$

where $P_{ij}^{n+1/2}$ is an intermediate variable.

4. Numerical Example

We applied the proposed model and solution algorithm to a rectangular walking platform with $x = 30$, $y = 20$. Pedestrians are only allowed to walk from the left boundary to the right one. There are two doors of the same width as $w = 4$ where pedestrians can enter the platform, as shown in Figure 2. Initially, there are no pedestrians in the platform. The boundary conditions are

$$P(x, 0, t) = 0, \qquad P(x, 20, t) = 0, \qquad P(0, [8, 12], t) = 0, \tag{4.1}$$
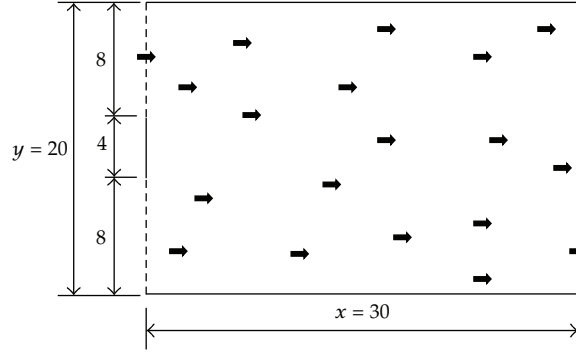
Figure 2: Schematic illustration of the one-way pedestrian flow in a platform. The length of the platform is 30 and the width is 20. The left dashed lines represent two entrances and the right one is exit. Solid lines are walls.

and the inputs are

$$P(0, d, t) = \frac{t}{1.5}, \quad t \in [0, 1.5],$$

$$P(0, d, t) = 1.0, \quad t \in (1.5, 3.5),$$

$$P(0, d, t) = \frac{(5 - t)}{1.5}, \quad t \in [3.5, 5],$$

$$P(0, d, t) = 0, \quad t > 5,$$

(4.2)

where $d = (0, 8) \cup (12, 20)$.

  We further assume r_1 to r_4 to be 0.70, 0.15, 0.0, and 0.15, respectively, and $\lambda = 0.045$ and $h = 0.05$.

  Figure 3 is snapshots of numerical solutions of the pedestrian flow at times $t = 1, 2, \ldots, 9$, respectively, to show the movement pattern of the pedestrians. The density increases steadily with the increase of entering flow and reaches its maximum at time $t = 5$. The density centered at either group is becoming less while the density between these two groups is becoming larger as the pedestrians are walking forward. For each group of pedestrians, density at the center is always larger than those in the surroundings. The reason is that the people around the block are much easier to disperse than those in the middle. As the time is close to $t = 9$, the density is approaching zero and only some late-entering or slow-walking people remain in the platform. From the snapshots, we can observe the phenomena of dispersion and advection of the pedestrian flow.

  To further illustrate the model, additional experiments were conducted with the whole left boundary, that is, $x = 0$, as the entrance. In addition, the inflow is supposed to be steady with $P(0, y, t) = 1.0$, where $y \in (0, 20)$ and $t \in (0, 30]$. Figure 4 plots the density along x at $t = 1, 2, \ldots, 8$, respectively. It can be observed that there is a sharp decrease in each curve, indicating that only a few pedestrians are fast walkers. The results are consistent with the phenomenon we may observe in reality that no matter how crowded a platform is, the density close to the exit is always less than the jam density.
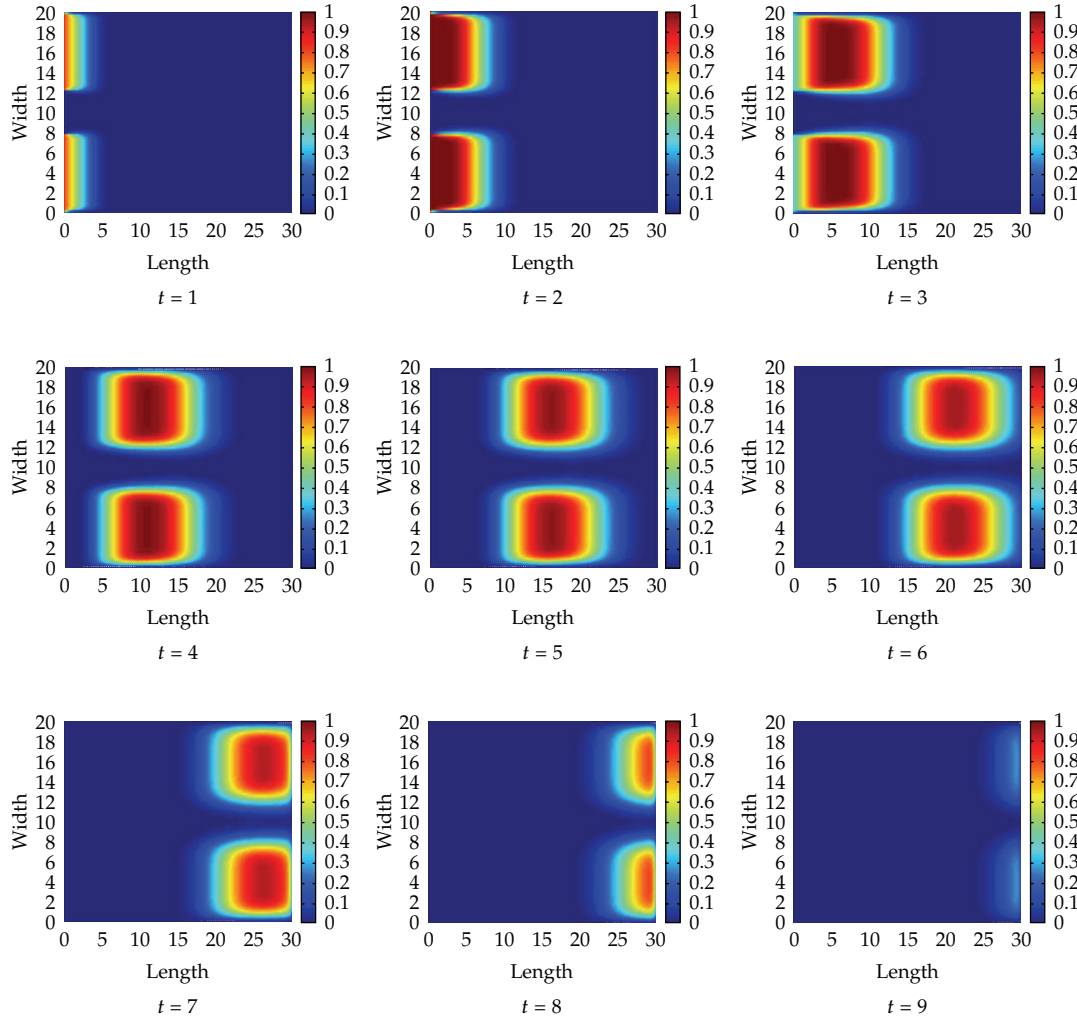
Figure 3: Density of pedestrian flow at different times.

To reveal the impact of direction choice behavior on the flow patterns, Figure 5 plots the average density of the platform along time under various scenarios where $r_1 = 0.80, 0.60, 0.40, 0.33$, respectively, and probabilities of left and right turns are $r_2 = r_4 = (1 - r_1)/2$ and walking backward is not allowed. It is shown that the time the flow becomes steady is significantly dependent on r_1. The larger r_1 is, the faster the flow reaches to a steady state. The numerical results coincide with actual pedestrian moving behavior. Moreover, a smaller value of r_1 leads to a lower density in the steady state.

Figure 6 illustrates the average density across the time under different entering flow intensity at PE $= 1.0, 0.8, 0.6, 0.4, 0.2$, respectively. It shows the steady density is only slightly lower than the input flow intensity. In addition, it is observed that no matter what intensity the inflow is, the time the flow reaches to its steady state remains almost the same.
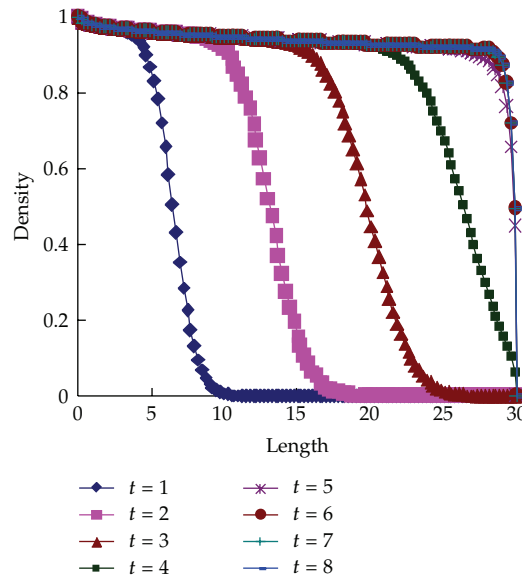
Figure 4: Density along x-axis at different times with $r_1 = 0.6$, $r_2 = 0.2$, $r_3 = 0.0$, and $r_4 = 0.2$.
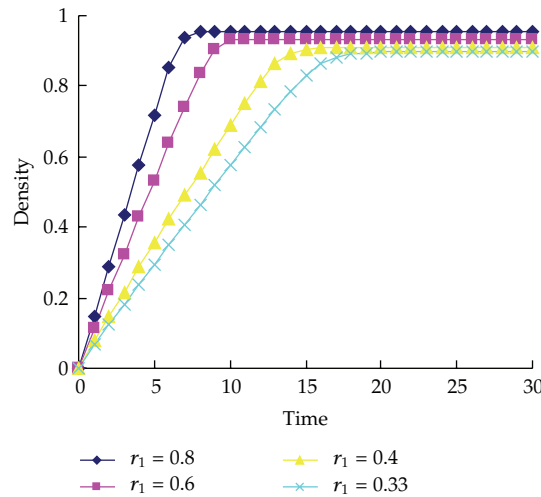

Figure 5: Average density of the platform along time with different r_1's.

5. Conclusion

This paper is an application of continuous-time random walks approach to pedestrian flow simulation. The model is capable of describing macroscopic phenomena such as forward moving and dispersion of pedestrian flow. In addition, by varying coefficients of the model, some microscopic phenomena such as route/direction choice behaviors can be replicated. To solve the model, a high-order compact scheme with the alternating direction implicit method is applied. Numerical results validated both the model and the numerical method.
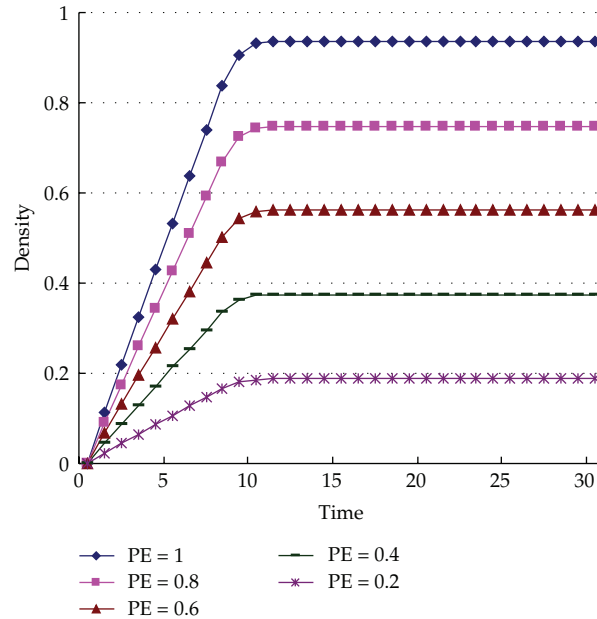
Figure 6: Average density with different entering flow intensity, where $r_1 = 0.6$, $r_2 = 0.2$, $r_3 = 0.0$, and $r_4 = 0.2$.

The model formulation in the paper only accounts for the distribution of the waiting time. In our future study, the probability distribution of jump length will be considered to further enhance the validity of the model. To make the model more practically applicable, we also plan to incorporate bi-direction flow and more realistic boundary conditions, such as input and output between platform and trains in platform.

Acknowledgment

References

[1] F. Weifeng, Y. Lizhong, and F. Weicheng, "Simulation of bi-direction pedestrian movement using a cellular automata model," *Physica A*, vol. 321, no. 3-4, pp. 633–640, 2003.
[2] W. G. Weng, T. Chen, H. Y. Yuan, and W. C. Fan, "Cellular automaton simulation of pedestrian counter flow with different walk velocities," *Physical Review E*, vol. 74, no. 3, Article ID 036102, 7 pages, 2006.
[3] V. J. Blue and J. L. Adler, "Cellular automata microsimulation for modeling bi-directional pedestrian walkways," *Transportation Research Part B*, vol. 35, no. 3, pp. 293–312, 2001.
[4] Y. F. Yu and W. G. Song, "Cellular automaton simulation of pedestrian counter flow considering the surrounding environment," *Physical Review E*, vol. 75, no. 4, Article ID 046112, 8 pages, 2007.
[5] L. Z. Yang, J. Li, and S. B. Liu, "Simulation of pedestrian counter-flow with right-moving preference," *Physica A*, vol. 387, no. 13, pp. 3281–3289, 2008.
[6] T. Nagatani, "Freezing transition in bi-directional CA model for facing pedestrian traffic," *Physics Letters, Section A*, vol. 373, no. 33, pp. 2917–2921, 2009.

[7] A. Varas, M. D. Cornejo, D. Mainemer et al., "Cellular automaton model for evacuation process with obstacles," *Physica A*, vol. 382, no. 2, pp. 631–642, 2007.

[8] M. Muramatsu, T. Irie, and T. Nagatani, "Jamming transition in pedestrian counter flow," *Physica A*, vol. 267, no. 3, pp. 487–498, 1999.

[9] M. Muramatsu and T. Nagatani, "Jamming transition of pedestrian traffic at a crossing with open boundaries," *Physica A*, vol. 286, no. 1, pp. 377–390, 2000.

[10] Y. Tajima, K. Takimoto, and T. Nagatani, "Scaling of pedestrian channel flow with a bottleneck," *Physica A*, vol. 294, no. 1-2, pp. 257–268, 2001.

[11] Y. Tajima and T. Nagatani, "Clogging transition of pedestrian flow in T-shaped channel," *Physica A*, vol. 303, no. 1-2, pp. 239–250, 2002.

[12] R. Jiang and Q. S. Wu, "The moving behavior of a large object in the crowds in a narrow channel," *Physica A*, vol. 364, pp. 457–463, 2006.

[13] D. Helbing and P. Molnár, "Social force model for pedestrian dynamics," *Physical Review E*, vol. 51, no. 5, pp. 4282–4286, 1995.

[14] W. J. Yu, R. Chen, L. Y. Dong, and S. Q. Dai, "Centrifugal force model for pedestrian dynamics," *Physical Review E*, vol. 72, no. 2, Article ID 026112, 7 pages, 2005.

[15] D. Yanagisawa and K. Nishinari, "Mean-field theory for pedestrian outflow through an exit," *Physical Review E*, vol. 76, no. 6, Article ID 061117, 9 pages, 2007.

[16] H. J. Huang and R. Y. Guo, "Static floor field and exit choice for pedestrian evacuation in rooms with internal obstacles and multiple exits," *Physical Review E*, vol. 78, no. 2, Article ID 021131, 9 pages, 2008.

[17] R. L. Hughes, "A continuum theory for the flow of pedestrians," *Transportation Research Part B*, vol. 36, no. 6, pp. 507–535, 2002.

[18] R. M. Colombo and M. D. Rosini, "Pedestrian flows and non-classical shocks," *Mathematical Methods in the Applied Sciences*, vol. 28, no. 13, pp. 1553–1567, 2005.

[19] L. F. Henderson, "On the fluid mechanics of human crowd motion," *Transportation Research*, vol. 8, no. 6, pp. 509–515, 1974.

[20] D. Helbing, "A fluid-dynamic model for the movement of pedestrians," *Complex Systems*, vol. 6, pp. 391–415, 1992.

[21] Y. Xia, S. C. Wong, and C. W. Shu, "Dynamic continuum pedestrian flow model with memory effect," *Physical Review E*, vol. 79, no. 6, Article ID 066113, 8 pages, 2009.

[22] E. Barkai, R. Metzler, and J. Klafter, "From continuous time random walks to the fractional Fokker-Planck equation," *Physical Review E*, vol. 61, no. 1, pp. 132–138, 2000.

[23] W. F. Spotz and G. F. Carey, "High-order compact scheme for the steady stream-function vorticity equations," *International Journal for Numerical Methods in Engineering*, vol. 38, no. 20, pp. 3497–3512, 1995.

[24] S. Karaa and J. Zhang, "High order ADI method for solving unsteady convection-diffusion problems," *Journal of Computational Physics*, vol. 198, no. 1, pp. 1–9, 2004.